

Tuning of the Photovoltaic Parameters of Molecular Donors by Covalent Bridging

Dora Demeter, Victorien Jeux, Philippe Leriche, Philippe Blanchard, Yoann Olivier, Jérôme Cornil, Riccardo Po, and Jean Roncali*

The synthesis of donor-acceptor molecules involving triarylamine and dicyanovinyl blocks is described. Optical and electrochemical results show that rigidification of the acceptor part of the molecule by a covalent bridge leads to a ca. 0.20 eV increase of the band gap due to a parallel increase of the lowest unoccupied molecular orbital level. A preliminary evaluation of these compounds as donor materials in organic solar cells shows that although this structural modification reduces the light-harvesting properties of the donor molecule, it nevertheless induces an increase of the efficiency of the resulting solar cells due to a simultaneous improvement of the open-circuit voltage and fill factor.

1. Introduction

Push-pull molecules built by connecting donor and acceptor blocks through a π -conjugating spacer (D- π -A) have been a focus of considerable interest for many years. Thus, a huge number of D- π -A chromophores for second order nonlinear optics have been developed during the 1990s.^[1] More recently, this class of compounds as well as other kinds of D/A combinations have received a renewal of interest motivated by their possible use as donor material in organic solar cells (OSCs).^[2] In fact, several recent works have shown that small push-pull systems can indeed lead to highly efficient OSCs.^[3–6] In this context, we recently reported D- π -A molecules involving triphenylamine as donor block and dicyanovinyl as acceptor connected by a thiophene ring and we have shown that the covalent bridging of the dicyanovinyl group with the adjacent

thiophene ring by a phenylene bridge leads to a considerable reduction of the band gap due to a large decrease of the LUMO level.^[6a] These effects lead to a significant improvement of the conversion efficiency of the resulting solar cells due in particular to a large extension of the spectral photo-response.

Our group has extensively investigated rigidification as an efficient synthetic principle for the synthesis of low band gap polymers and oligomers or D- π -A NLO-phores.^[7] In the specific case of molecular donors for OSCs, this approach can represent an interesting tool for the modulation

of the electronic properties of the system at a moderate cost in terms of structural complexification and increase of molecular weight.

In our continuing interest in the systematic analysis of structure-properties relationships of small molecular donors for OSCs, we report here on the effects of covalent rigidification of two D- π -A molecules (**1** and **3**) by covalent bridging of the electron acceptor thienyl-dicyanovinyl group by an ethylene bridge (**2** and **4**) (Scheme 1).

2. Results and Discussion

The synthesis of compounds **1–4** is depicted in Scheme 2. 4-bromo-*N,N*-bis(4-methoxyphenyl)aniline,^[8] 2-tributylstannyl-5-[*N,N*-bis(4-methoxyphenyl)]thiophenamine (**12**),^[9] 5-(4-(bis(4-methoxyphenyl) amino)-phenyl)thiophene-2-carbaldehyde (**5**)^[10] and 2-bromo-4,5-dihydrocyclopenta[b]thiophen-6-one (**10**)^[11] have been prepared according to literature procedures. 4-tributylstannyl-*N,N*-bis(4-methoxyphenyl)aniline (**11**)^[12] was prepared by treatment of 4-bromo-*N,N*-bis(4-methoxyphenyl)aniline with butyllithium and reaction with tributylstannyl chloride. The intermediate ketones or aldehydes **6**, **7** and **8** have been synthesized by Stille coupling of the appropriate stannylated agents **11** and **12** with 2-bromo-5-formyl thiophene **9**, and bromo-ketone **10**. Finally the four target compounds **1–4** have been obtained by Knoevenagel condensation of carbonyl compounds **5–8** with malonodinitrile in the presence of triethylamine. All target compounds have been satisfactorily characterized by usual spectrometric and analytical techniques.

The optical properties of the target compounds have been investigated by UV-vis absorption spectroscopy of solutions and of thin films spin-cast on glass from chloroform solutions.

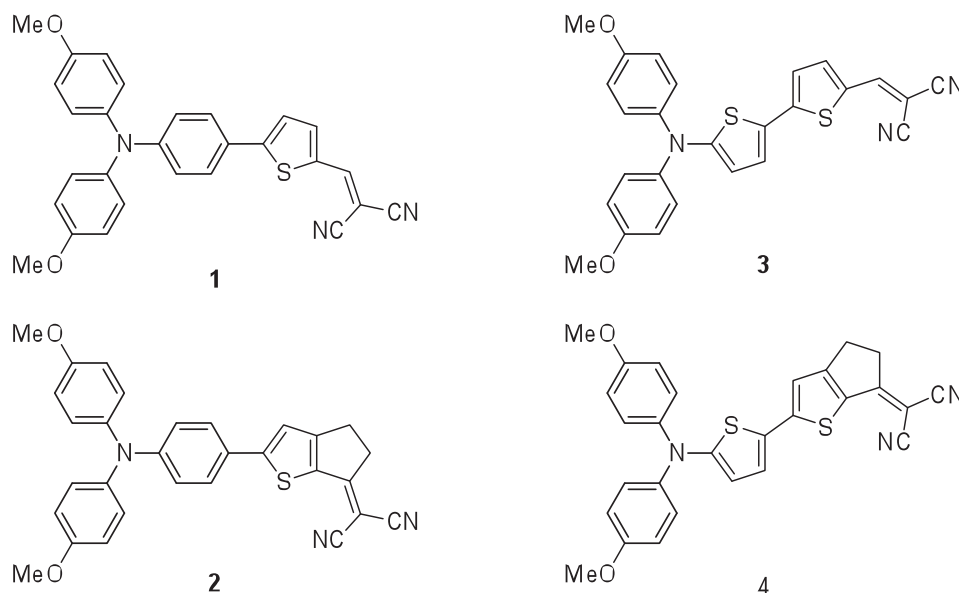
Dr. D. Demeter, V. Jeux, Prof. P. Leriche,
Dr. P. Blanchard, Dr. J. Roncali
Group Linear Conjugated Systems
CNRS UMR 6200, MOLTECH-Anjou
University of Angers 2 Bd Lavoisier
49045 Angers, France
E-mail: jeanroncali@gmail.com

Dr. Y. Olivier, Dr. J. Cornil
Laboratory for Chemistry of Novel Materials
University of Mons
Place du Parc, 7000, Mons, Belgium

Dr. R. Po
Centro ricerche per le energie non convenzionali Istituto
ENI Donegani ENI S.p.A., via G. Fauser 4, 28100 Novara, Italy



DOI: 10.1002/adfm.201300427



Scheme 1. Structure of the donor molecules.

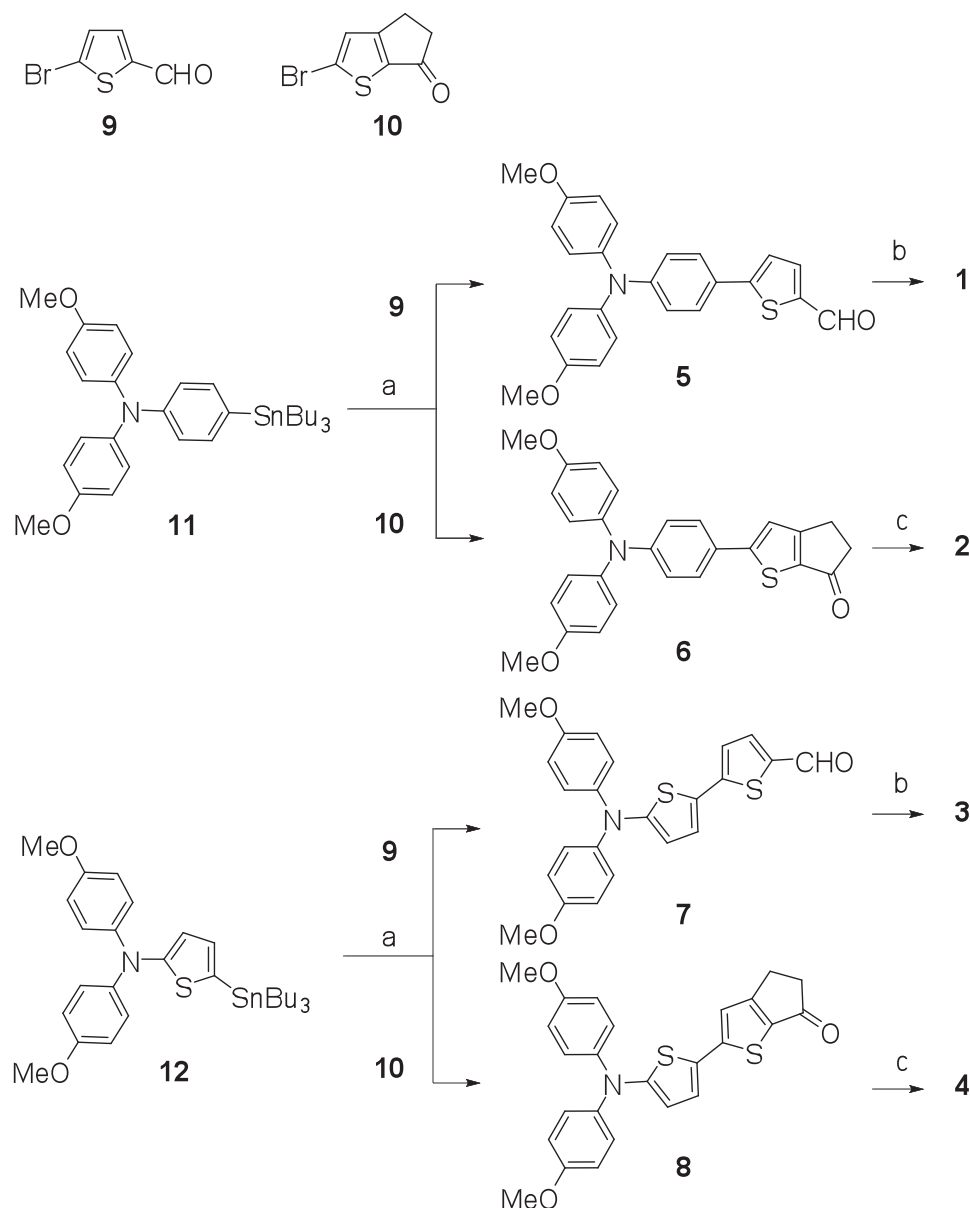
Figure 1 shows the absorption spectra of the four compounds in methylene chloride and as thin film spin-cast on glass from chloroform solutions. The spectrum of all compounds presents a first absorption band in the 300–400 nm region and a second band at longer wavelengths assigned to an internal charge transfer (ICT).^[13] Comparison of the data for compounds 1 and 2 to those of 3 and 4 shows that replacing the inner phenyl ring of TPA by a thiophene unit leads to a ca. 50 nm red shift of λ_{max} . This difference can be attributed to the smaller aromatic resonance energy of thiophene which allows a better electron delocalization.^[14] For both starting structures the bridge induces a 23–24 nm hypsochromic shift of λ_{max} corresponding to a 0.15–0.20 eV increase of the HOMO-LUMO gap.

The optical band gap of the compounds (E_g) has been estimated from the long wavelength absorption edge of the absorption spectrum of the films. The data in Table 1 confirm that for both systems, the materials derived from the bridged molecules present larger E_g values than their open analogs. For many conjugated systems, the passage from solution to the solid-state is generally accompanied with a broadening of the absorption bands and a red shift of the absorption maximum due to intermolecular interactions in the solid. While such a behavior is also observed for the open compounds 1 and 3, the spectra of films of the bridged compounds 2 and 4 reveal two noticeable differences. Firstly the spectrum of the films presents a few nanometers hypsochromic shift of λ_{max} compared to solution spectra (Table 1). This unexpected behavior suggests that bridging induces a different molecular organization in the solid state with the possible formation of H-aggregates. On the other hand, for the bridged compounds the broadening of the absorption bands in the solid-state is more limited than for open systems which could reflect a narrower distribution of conformers and/or vibrational states in materials derived from the bridged systems, but this question requires further investigations.

The thermal data in Table 1 show that all compounds present relatively low melting points and high decomposition temperatures suggesting that the compounds can probably be processed by vacuum deposition techniques.

Cyclic voltammetry (CV) has been performed in methylene chloride in the presence of Bu_4NPF_6 as supporting electrolyte. The CV of the four compounds presents a first reversible one-electron oxidation process with an anodic peak potential (E_{pa}) around 0.75 V followed by a second anodic peak around 1.40 V. Comparison of the CV data for compounds 1 with 3, and 2 with 4 shows that replacement of a phenyl ring by a thiophene unit in the triarylamine block produces a 30–40 mV negative shift of E_{pa} consistent with optical data. All compounds undergo an irreversible reduction at a cathodic peak potential (E_{pr}) although close examination of the CV traces shows that bridging seems to slightly improve the reversibility of the process (Figure 2). On the other hand, pairwise comparison of the data for compound 1 and 2, and 3 and 4 shows that bridging has practically no effect on E_{pa} but leads to a 0.20 V negative shift of E_{pr} (Table 2). This indicates the bridge raises the energy level of the LUMO without affecting the HOMO level. These results show that the increase of E_g produced by the bridge is due exclusively to a destabilization of the LUMO level and they suggest that the HOMO and LUMO orbitals are strongly localized on the donor and acceptor parts of the molecule respectively. The energy levels of HOMO and LUMO were determined from the onset of the oxidation and reduction waves respectively using an offset of 4.99 eV for the saturated calomel reference electrode (SCE) vs vacuum level. The HOMO-LUMO gaps (ΔE) derived from these values agree well with optical data and that the bridge increases the energy gap.

In order to gain further insight into the effect of covalent bridging on the electronic properties, quantum chemical calculations based on density functional methods have been performed with the Gaussian 09 package for analogs of



Scheme 2. Synthesis of donors **1–4**. a) $\text{Pd}(\text{PPh}_3)_4$, toluene; b) malonodinitrile, Et_3N , chloroform; c) malonodinitrile, Et_3N , dichloroethane.

compounds **1** and **2** devoid of methoxy substituents on the TPA unit. Becke's three-parameter gradient-corrected functional (B3LYP) with 6-31G(d,p) basis was used to optimize the geometry and to compute the electronic structure. Except for the two outermost phenyl units of TPA, both molecules exhibit a quasi-planar structure. The dicyanovinyl moiety of **1** and **3** adopts a *syn* conformation relative to the sulfur atom of the thiophene ring while this geometry is imposed by the bridge for compound **2** and **4**. With reference to the open compound **1** and **3**, the bridge produces a significant increase of the LUMO level (0.25 eV) but only a small increase of the HOMO (0.05 eV) (Table 3). This exclusive effect on the LUMO level is consistent with a LUMO strongly localized on the thienyl-dicyanovinyl

block and the HOMO on the triarylamine unit (Figure 3). The calculated values of the HOMO and LUMO level for the four donors are in good qualitative agreement with experimental data with in particular the lower ΔE values of compounds **3** and **4** with a diphenylthienylamine donor block, and the ca. 0.20 eV destabilization of the LUMO level with a parallel increase of ΔE for the bridged systems **2** and **4**. The above experimental and theoretical results suggest that besides the rigidification of the molecule, the covalent bridge induces a destabilization of the LUMO by the inductive electron-releasing effect of the two methylene groups of the bridge.^[7d]

The efficiency of the four D-A compounds as donor material for photovoltaic conversion has been evaluated on bilayer

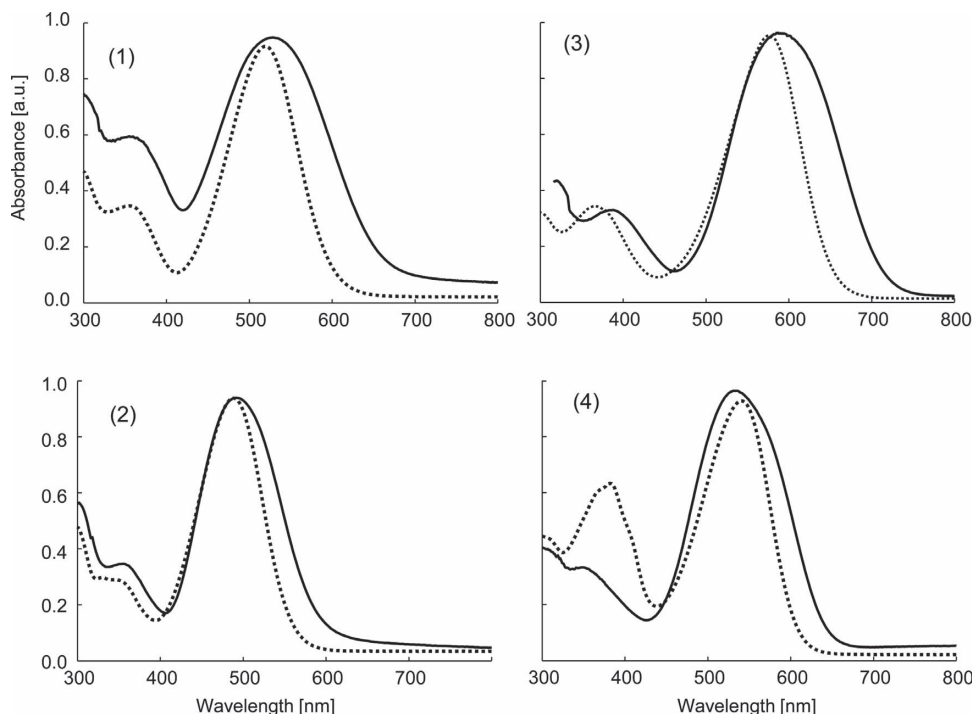


Figure 1. Normalized UV-Vis absorption spectra of compounds **1–4** in methylene chloride (dotted lines) and as thin films spin-cast on glass from chloroform solutions.

planar hetero-junction (PHJ) solar cells of 0.28 cm² active area. Although solution-processed or vacuum deposited bulk hetero-junctions are known to be more efficient, such cells require the optimization of many experimental variables. Therefore basic bilayer PHJ cells appear more appropriate and more reliable for a first analysis of structure-properties relationships. Consequently the quoted results must be considered as minima and it is clear that much better performances can be obtained with more advanced device architectures.^[15]

The test devices were fabricated by spin-casting a ca. 35-nm-thick donor film from chloroform solutions (ca. 5 mg mL⁻¹) on ITO substrates pre-coated by a 40-nm layer of PEDOT:PSS. A 30-nm layer of C₆₀ was then vacuum deposited and the devices were completed by deposition of a 100 nm aluminium electrode. Each batch consists of three or four slides with two cells of 0.28 cm² on each slide. For all compounds, application of a

Table 1. UV-vis absorption data for compounds **1–4** in methylene chloride solution and as thin films spun-cast on glass from chloroform solutions.

Compd	$\lambda_{\text{max}}^{\text{(CT)}}$ [nm]	$\log \epsilon_{\text{(CT)}}$ [M ⁻¹ cm ⁻¹]	$\lambda_{\text{max}}^{\text{a)}$ [nm]	$E_{\text{g}}^{\text{a)}$ [eV]	<i>Mp</i> [°C]	<i>Td</i> [°C]
1	519	4.44	526	1.87	66	306
2	494	4.63	490	2.10	124	315
3	576	4.53	588	1.77	162	295
4	542	4.39	533	1.92	150	309

^{a)} on films.

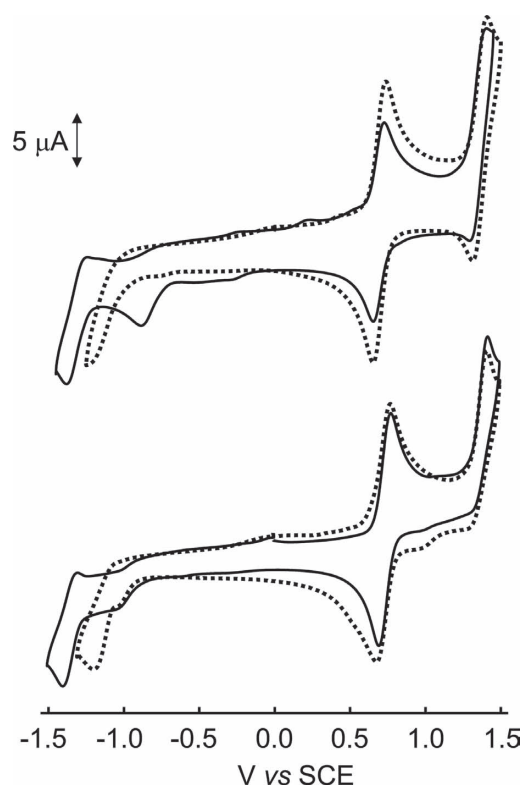


Figure 2. Cyclic voltammograms recorded in 0.10 M Bu₄NPF₆/CH₂Cl₂, scan rate 100 mV s⁻¹. Top: dotted line (**1**), solid line (**2**); Bottom: Dotted line (**3**), solid line (**4**).

Table 2. Cyclic voltammetry data for compounds **1–4** in 0.10 M Bu₄NPF₆/CH₂Cl₂, scan rate 100 mV s^{−1}, reference SCE.

Compd	<i>E</i> _{pa} ¹ [V]	<i>E</i> _{pr} ¹ [V]	<i>E</i> _{HOMO} [eV]	<i>E</i> _{LUMO} [eV]	Δ <i>E</i> [eV]
1	0.77	−1.18	−5.67	−3.81	1.86
2	0.77	−1.38	−5.67	−3.59	2.08
3	0.74	−1.17	−5.63	−3.82	1.81
4	0.73	−1.37	−5.63	−3.62	2.01

Table 3. Calculated HOMO and LUMO levels of compounds **1–4**.

Compd	HOMO [eV]	LUMO [eV]	Δ <i>E</i> [eV]
1	−5.34	−2.76	2.58
2	−5.29	−2.51	2.79
3	−5.27	−2.79	2.49
4	−5.22	−2.57	2.65

5 min thermal treatment at 120 °C was found to significantly improve the power conversion efficiency (*PCE*) through the increase of the short-circuit current density (*J*_{sc}), open-circuit voltage (*V*_{oc}) or filling factor (*FF*).

Attempts to observe some thermally induced material reorganization with eventual crystallization using X-ray diffraction and UV-vis absorption spectroscopy on pure donor films remained unsuccessful. This result suggests that the observed increase of *PCE* may be caused by a thermally induced interpenetration of the D and A materials leading to an extension of the D/A interfacial contact zone. Although this hypothesis needs to be confirmed, it is consistent with the higher efficiency of mixed co-evaporated cells compared to simple bilayer cells.^[4b,5a,16]

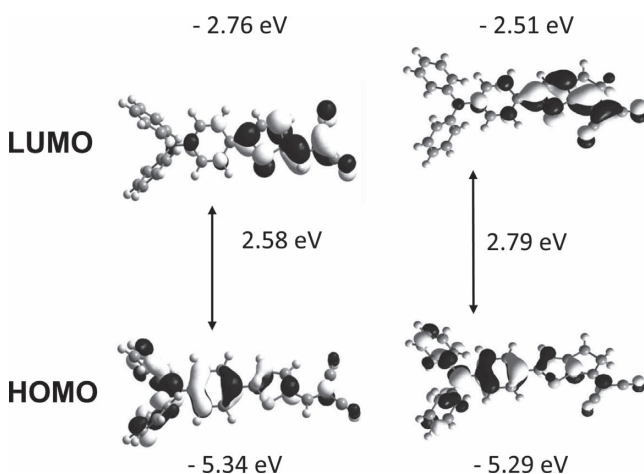


Figure 3. HOMO and LUMO orbitals of compound **1** (left) and **2** (right); methoxy groups are omitted.

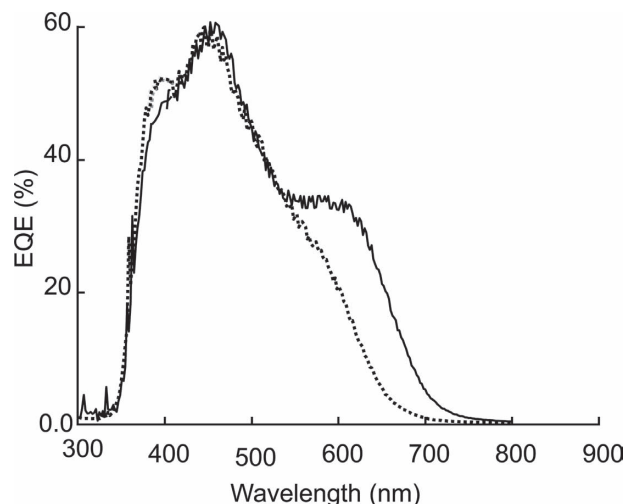


Figure 4. External quantum efficiency of PHJ cells donor/C₆₀ under monochromatic irradiation. Solid line (donor **3**) dotted line (donor **4**).

Figure 4 shows as representative example, the external quantum efficiency (*EQE*) responses of the cells based on compounds **3** and **4** under monochromatic illumination. These spectra clearly show that the bridging of the donor molecule leads to a restriction of the spectral response in the long wavelength region, as could be anticipated from the UV-vis absorption spectra. **Figure 5** shows the current density vs voltage curves of the four types of cells under white light illumination with a power light intensity of 90 mW cm^{−2}. The cell based on compound **1** gives a *J*_{sc} of 5.88 mA cm^{−2} and a *V*_{oc} of 0.70 V which combined with a *FF* of 30% leads to a *PCE* of 1.47% (**Table 4**).

The results show that as expected, for both bridged and open donors, replacement of a phenyl ring by a thiophene leads to a decrease of *V*_{oc} due to the increase of the HOMO level of the donor and to an increase of *J*_{sc} due to the extension of the spectral response that result in an increase of *PCE* to 1.84%. The *J*–*V* curves of **Figure 5** and the data in **Table 4** show that for both systems, the bridging of the donor molecule produces identical effects. As suggested by the *EQE* spectra, a noticeable reduction of *J*_{sc} is observed. However, in both cases the bridge induces a significant increase of *FF* and *V*_{oc} that result in a noticeable improvement of *PCE* from 1.47% for compound **1** to 2.23% for compound **2**.

The increase of *V*_{oc} upon bridging is particularly intriguing in view of the identical HOMO levels of the bridged and non-bridged compounds. This result could reflect a modification of the interfacial dipole in the D/A junction due to a specific packing arrangement and/or orientation of the donor molecules. We have recently reported a similar phenomenon produced by de-symmetrization of donors based on A-D-A molecules.^[17] Similarly we have no definitive explanation for the observed improvement of *FF*. A modification of molecular packing leading to a better charge collection at the donor/electrode interface or improved charge-transport could be invoked. These questions require further investigations and will be discussed in future publications.

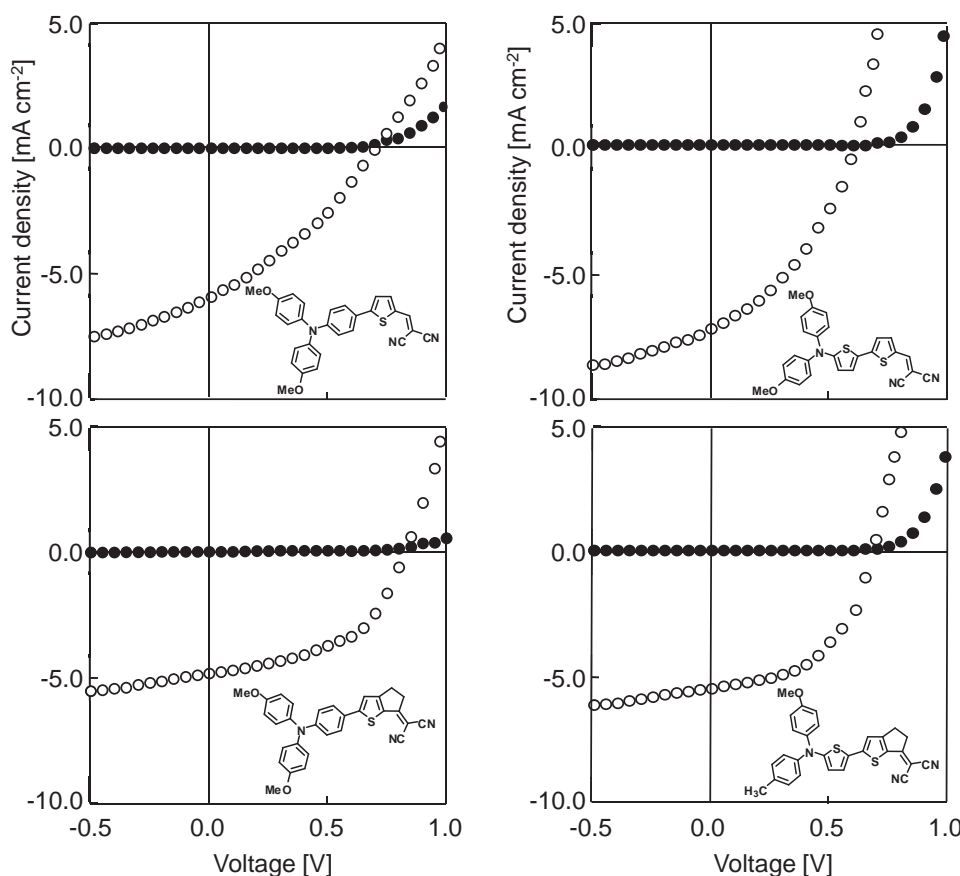


Figure 5. Current density vs voltage curves for bi-layer planar heterojunction cells donor/ C_{60} under white light illumination at a power density of 90 mW cm^{-2} . Top: left 1, right 3, bottom left 2, right 4.

3. Conclusion

The effects of partial rigidification of small push-pull molecules based on triarylamine donor blocks and the thienyldicyanovinyl acceptor group have been investigated. Optical and electrochemical results clearly demonstrate that the covalent bridging of the dicyanovinyl group with the adjacent thienyl ring does not affect the HOMO level but produces a ca. 0.20 eV increase of the band gap due to an equivalent increase of the LUMO level.

Table 4. Photovoltaic parameters obtained after 5 min thermal treatment at 120°C for bi-layer planar heterojunction cells donor/ C_{60} based on donors 1–4 under white light illumination at a power density of 90 mW cm^{-2} .

Compd	V_{oc} [V]	J_{sc} [mA cm^{-2}]	FF [%]	PCE [%]
1	0.70	5.88	32	1.47
2	0.82	4.87	50	2.23
3	0.59	7.23	39	1.84
4	0.67	5.50	52	2.12

A preliminary evaluation of the performances of the molecules as donor material in basic bilayer solar cells has been carried out. The results obtained on two molecular structures show that covalent bridging produces counter-acting effects namely a reduction of the light-harvesting properties and hence a decrease of the cell current intensity and an improvement of the open-circuit voltage and fill factor that result in a significant increase of efficiency.

While it is evident that the increase of the band gap is a direct consequence of the structural modification of the molecule, the origin of the increase of the voltage and fill factor is clearly intermolecular and could involve changes in the molecular packing, molecular orientation and interfacial dipole at the D/A heterojunction. A detailed understanding of these phenomena is beyond the scope of this work and will require further investigations, with in particular further efforts to crystallize some derivatives of these structures. However, in view of the importance of the dicyanovinyl group in the design of active materials for OSCs,^[4–6,13,17–19] these results can already contribute to provide new guidelines for the design of active materials for OSCs. Work aiming at the extension of these concepts to other structures is now in progress and will be reported in future publications.

4. Experimental Section

General: NMR spectra were recorded with a Bruker AVANCE III 300 (^1H , 300 MHz and ^{13}C , 75 MHz) or Bruker AVANCE DRX 500 (^1H , 500 MHz and ^{13}C , 125 MHz). Chemical shifts are given in ppm relative to TMS. IR spectra were recorded on a Bruker spectrometer Vertex 70 and UV-Vis spectra with a Perkin Elmer 950 spectrometer. Melting points are uncorrected. Matrix Assisted Laser Desorption/Ionization was performed on MALDI-TOF MS BIFLEX III Bruker Daltonics spectrometer using dithranol as matrix. Cyclic voltammetry was performed in 0.10 M $\text{Bu}_4\text{NPF}_6/\text{CH}_2\text{Cl}_2$ (HPLC grade). Solutions were degassed by nitrogen bubbling prior to each experiment. Experiments were carried out in a one-compartment cell equipped with platinum electrodes and a saturated calomel reference electrode (SCE) using a Biologic SP-150 potentiostat with positive feedback compensation. Elemental analyses were performed with a thermo-electron instrument. Column chromatography purifications were carried out on Acros silica gel Si 60 (35–70 mm). DSC and TGA were performed with TA Instruments.

Device Preparation: Indium-tin oxide coated glass slides of 24 mm \times 25 mm \times 1.1 mm with a surface resistance of 10 Ω/\square were purchased from Kintec company. Part of the ITO layer was etched away with 37% HCl. The ITO electrodes were then cleaned in ultrasonic bath successively with Deconex (from VWR international GmbH), distilled water (15.3 M Ω cm^{-1}), acetone, ethanol and distilled water again for 10 min each and dried in an oven at 100°C. The electrodes were then modified by a spin-cast layer of PEDOT:PSS (Clevios P VP, AI 4083 (HC-Starck) filtered through a 0.45 μm membrane just prior use). Spin-casting was achieved at 5000 rpm ($r = 10$ s, $t = 60$ s), and the electrode was then dried at 130°C for 15 min. Films of donor materials of 30–35 nm thickness were spun-cast in atmospheric conditions from chloroform solutions containing 5 mg mL^{-1} . Chloroform (HPLC grade) was distilled over P_2O_5 before use. After film deposition the devices were introduced in an argon glovebox (200B, MBraun) equipped with a vacuum chamber and a 30 nm film of C_{60} fullerene (99+%) (MER Corporation) and a 100-nm-thick aluminium electrode were thermally evaporated on top of the donor film under a pressure of 2×10^{-6} mbar through a mask defining two cells of 6.0 mm diameter (0.28 cm^2) on each ITO electrode. C_{60} (99+%) was purchased from MER Corporation and used as received.

The J - V curves of the devices were recorded in the dark and under illumination using a Keithley 236 source-measure unit and a home-made acquisition program. The light source was an AM1.5 Solar Constant 575 PV simulator (Steuernagel Lichttechnik, equipped with a metal halogen lamp). The light intensity was measured by a broad-band power meter (13PEM001, Melles Griot). The devices were illuminated through the ITO electrode side. The efficiency values reported here are not corrected for the possible spectral mismatch of the solar simulator. External quantum efficiency (EQE) was measured using a halogen lamp (Osram) with an Action Spectra Pro 150 monochromator, a lock-in amplifier (Perkin-Elmer 7225) and a S2281 photodiode (Hamamatsu).

Synthesis: **4-tributylstannyl-N,N-bis(4-methoxyphenyl)aniline (11).** To a solution of 4-bromo-N,N-bis(4-methoxyphenyl)aniline (0.25 g, 0.65 mmol) in 10 mL of THF at -78°C , $n\text{-BuLi}$ (2.5 M in hexane, 0.3 mL, 0.72 mmol) is added dropwise. After 1.5 h of stirring at the same temperature, tributylstannyl chloride (0.2 mL, 0.72 mmol) is added and the mixture is slowly warmed to room temperature and stirred for 12 h. After dilution with diethyl ether, a saturated solution of NaF is added and the mixture is stirred for 1 h. The precipitate is filtered off using celite and the filtrate is washed with a saturated solution of NaHCO_3 then with water. After drying over MgSO_4 , the solvent is evaporated and the product is used in the next step without further purification. ^1H NMR (300 MHz, CDCl_3): 7.24 (d, 2H, $J = 8.4$ Hz), 7.08 (d, 4H, $J = 9$ Hz), 6.89 (d, 2H, $J = 8.4$ Hz), 6.83 (d, 4H, $J = 9$ Hz), 3.78 (s, 6H), 1.64–1.50 (m, 6H), 1.39–1.24 (m, 12H), 0.94–0.84 (m, 9H).

2-[4-(bis(4-methoxyphenyl)amino)phenyl]-4H-cyclopenta[b]thiophen-6(5H)-one (6). A mixture of compound **10** (0.14 g, 0.64 mmol), Stille reagent **11** (0.45 g, 0.76 mmol), and $\text{Pd}(\text{PPh}_3)_4$ (74 mg, 10 mol%) in 20 mL of anhydrous toluene is refluxed for 20 h. After concentration, the residue is dissolved in CH_2Cl_2 and the organic phase is washed

with aqueous NaHCO_3 and water. After drying over MgSO_4 and solvent removal the residue is chromatographed on silica gel using methylene chloride as eluent to give 0.13 g (47%) of a yellowish compound. ^1H NMR (500 MHz, CDCl_3): 7.42 (d, 2H, $J = 8.5$ Hz), 7.10 (d, 4H, $J = 8.5$ Hz), 7.09 (s, 1H), 6.89 (d, 2H, $J = 8.5$ Hz), 6.86 (d, 4H, $J = 9$ Hz), 3.80 (s, 6H), 3.02–2.98 (m, 2H), 2.92–2.90 (m, 2H). ^{13}C NMR (125 MHz, CDCl_3): 196.9, 169.7, 160.6, 156.4, 149.8, 139.8, 137.5, 127.1, 126.9, 124.7, 119.1, 117.7, 114.7, 55.4, 40.4, 24.1. MS MALDI: 442.08. HRMS: calcd 442.14714, found 442.14694.

5'-(bis(4-methoxyphenyl)amino)-[2,2'-bithiophene]-5-carbaldehyde (11). A mixture of aldehyde **9** (0.54 g, 2.85 mmol), Stille reagent **12** (1.14 g, 1.9 mmol) and $\text{Pd}(\text{PPh}_3)_4$ (110 mg, 5 mol%) in 20 mL of anhydrous toluene is refluxed for 20 h. After concentration, the residue is dissolved in CH_2Cl_2 and the organic phase is washed twice with aqueous NaHCO_3 and water. After drying over MgSO_4 and solvent removal the residue is chromatographed on silica gel using methylene chloride as eluent to give (0.53 g, 66%) of a yellowish compound. M.p. = 104–105 $^\circ\text{C}$. IR (neat): $\nu = 1648$ cm^{-1} ($\text{C}=\text{O}$), ^1H NMR (300 MHz, CDCl_3): 9.77 (s, 1H), 7.57 (d, 1H, $J = 3.9$ Hz), 7.16 (d, 4H, $J = 9$ Hz), 7.08 (d, 1H, $J = 4.2$ Hz), 6.96 (d, 1H, $J = 4.2$ Hz), 6.86 (d, 4H, $J = 9$ Hz), 6.28 (d, 1H, $J = 3.9$ Hz), 3.81 (s, 6H). ^{13}C NMR (75 MHz, CDCl_3): 182.1, 156.9, 156.7, 148.7, 140.3, 139.6, 137.8, 126.5, 125.7, 123.9, 121.8, 114.7, 113.6, 55.5. Anal (calcd): C 65.57 (65.53), H 4.46 (4.54), N 3.29 (3.32), S 15.20 (15.21).

2-(5-(bis(4-methoxyphenyl)amino)thiophen-2-yl)-4H-cyclopenta[b]thiophen-6(5H)-one-8. A mixture of compound **10** (0.16 g, 0.74 mmol), Stille reagent **12** (0.60 g, 0.88 mmol) and $\text{Pd}(\text{PPh}_3)_4$ (84 mg, 10 mol%) in 20 mL of anhydrous toluene is refluxed for 20 h. After concentration, the residue is dissolved in CH_2Cl_2 and the organic phase is washed twice with aqueous NaHCO_3 and water. After drying over MgSO_4 and solvent removal the residue is chromatographed on silica gel using methylene chloride as eluent to give (0.21 g, 64%) of an orange compound. ^1H NMR (500 MHz, CDCl_3): 7.16 (d, 4H, $J = 8.5$ Hz), 7.05 (d, 1H, $J = 4$ Hz), 6.88 (d, 4H, $J = 9$ Hz), 6.81 (s, 1H), 6.27 (d, 1H, $J = 4$ Hz), 3.80 (s, 6H), 2.95–2.93 (m, 2H), 2.91–2.89 (m, 2H). ^{13}C NMR (125 MHz, CDCl_3): 196.4, 169.6, 156.6, 153.8, 140.3, 136.6, 125.69, 125.62, 124.3, 117.2, 114.7, 113.5, 55.4, 40.4, 24.1. MS MALDI: 447.06. HRMS ESI: calcd 447.09628; found 447.09595.

2-(5-(4-(bis(4-methoxyphenyl)amino)phenyl)thiophen-2-yl)methylene malononitrile-1. Aldehyde (**5**). (0.11 g, 0.26 mmol) is dissolved in a solution of malonitrile (0.05 g, 0.78 mmol) in dry CHCl_3 (50 mL), three drops of triethylamine are added and the resulting solution is stirred 24 h at room temp. The mixture is diluted with CH_2Cl_2 , washed with a solution of sodium hydroxide (1 M), water and brine. After removal of solvent the residue is chromatographed on silica gel using methylene chloride as eluent to give 0.09 g (79%) of a dark solid. M.p.: 66–68 $^\circ\text{C}$. IR (neat): $\nu = 2217$ cm^{-1} ($\text{C}\equiv\text{N}$). ^1H NMR (300 MHz, CDCl_3): 7.71 (s, 1H), 7.65 (d, 1H, $J = 4.2$ Hz), 7.47 (d, 2H, $J = 9$ Hz), 7.28 (d, 1H, 4.2 Hz), 7.10 (d, 4H, $J = 8.7$ Hz), 6.87 (d, 6H, $J = 9$ Hz), 3.82 (s, 6H). ^{13}C NMR (75 MHz, CDCl_3): 157.8, 156.8, 150.7, 150.2, 140.5, 139.4, 132.6, 127.5, 127.4, 123.1, 122.7, 118.8, 114.9, 114.7, 113.8, 74.3, 55.5. HRMS ESI: calcd 463.13545; found 463.13481.

2-(2-(4-(bis(4-methoxyphenyl)amino)phenyl)-4H-cyclopenta[b]thiophen-6(5H)-ylidene)malononitrile (2). Ketone **6** (0.15 g, 0.33 mmol) is dissolved in a solution of malonitrile (0.15 g, 0.33 mmol) in dry 1,2-dichloroethane (50 mL), three drops of triethylamine are added and the solution is 24 h at 90 $^\circ\text{C}$ under inert atmosphere. The mixture is cooled to room temp, diluted with CH_2Cl_2 , washed with water and brine. After removal of solvent the residue is chromatographed on silica gel using methylene chloride as eluent to give 30 mg, (19%) of a reddish solid. M.p.: 124–126 $^\circ\text{C}$. IR (neat): $\nu = 2213$ cm^{-1} ($\text{C}\equiv\text{N}$). ^1H NMR (500 MHz, CDCl_3): 7.43 (d, 2H, $J = 8.7$ Hz), 7.10 (d, 4H, $J = 9$ Hz), 7.09 (s, 1H), 6.90 (d, 2H, $J = 8.7$ Hz), 6.87 (d, 4H, $J = 9$ Hz), 3.80 (s, 6H), 3.02–2.99 (m, 2H), 2.94–2.91 (m, 2H). ^{13}C NMR (125 MHz, CDCl_3): 172.1, 167.9, 163.6, 158.8, 150.7, 139.4, 136.5, 127.4, 127.3, 123.6, 118.7, 116.9, 114.9, 114.3, 66.3, 55.4, 38.1, 27.4. MS MALDI: 489.12. HRMS: calcd 489.15110, found 489.15055.

2-((5'-(bis(4-methoxyphenyl)amino)-[2,2'-bithiophen]-5-yl)methylene malononitrile (3). Aldehyde **7** (0.14 g, 0.34 mmol) is dissolved in a

solution of malonitrile (0.068 g, 1.02 mmol) in dry CHCl_3 (50 mL) and then three drops of triethylamine are added and the resulting solution is stirred at room temperature. After 24 h, the reaction mixture is diluted with CH_2Cl_2 , washed with a solution of sodium hydroxide (1M), water and brine. After removal of solvent the residue is chromatographed on silica gel using methylene chloride as eluent to afford a dark solid (0.10 g, 65%). M.p.: 162–164 °C, IR (neat): $\nu = 2215 \text{ cm}^{-1}$ ($\text{C}\equiv\text{N}$). ^1H NMR (300 MHz, CDCl_3): 7.63 (s, 1H), 7.49 (d, 1H, $J = 4.5 \text{ Hz}$), 7.19 (m, 5H), 6.95 (d, 1H, 4.2 Hz), 6.88 (d, 4H, $J = 9 \text{ Hz}$), 6.24 (d, 1H, $J = 4.2 \text{ Hz}$), 3.82 (s, 6H) ^{13}C NMR (75 MHz, CDCl_3): 159.4, 157.4, 151.6, 149.3, 140.9, 139.7, 131.24, 128.3, 126.4, 121.8, 121.7, 114.9, 114.6, 114.2, 112.2, 72.5, 55.5. HRMS ESI calculated 470.09969; found 470.09882.

2-(2-(5-(bis(4-methoxyphenyl)amino)thiophen-2-yl)-4H-cyclopenta[b]thiophen-6(5H)-ylidene)malononitrile (4). Ketone **8** (0.12 g, 0.26 mmol) is dissolved in a solution of malonitrile (0.12 g, 1.87 mmol) in dry 1,2-dichloroethane (20 mL), three drops of triethylamine are added and the resulting solution is stirred at 90 °C under inert atmosphere for 24 h. The reaction mixture is cooled to room temperature, diluted with CH_2Cl_2 , washed with water and brine. After removal of solvent the residue is chromatographed on silica gel using methylene chloride as eluent to afford a violet solid (30 mg, 23%). M.p.: 150–152 °C. IR (neat): $\nu = 2214 \text{ cm}^{-1}$ ($\text{C}\equiv\text{N}$). ^1H NMR (300 MHz, CDCl_3): 7.17 (d, 4H, $J = 9 \text{ Hz}$), 7.05 (d, 1H, $J = 4 \text{ Hz}$), 6.87 (d, 4H, $J = 9 \text{ Hz}$), 6.82 (s, 1H), 6.28 (d, 1H, $J = 4 \text{ Hz}$), 3.80 (s, 6H), 2.99–2.93 (m, 2H), 2.91–2.88 (m, 2H). ^{13}C NMR (125 MHz, CDCl_3): 171.1, 167.9, 159.0, 157.3, 157.0, 139.7, 135.1, 127.7, 126.3, 122.2, 115.8, 114.9, 114.6, 114.5, 112.0, 65.0, 55.5, 38.1, 27.1. MS MALDI: 495.05. HRMS: calcd 495.10752; found 495.10690.

Acknowledgements

Y.O. and J.C. are FNRS research fellows.

Received: February 2, 2013

Revised: March 5, 2013

Published online: April 9, 2013

- [1] a) D. R. Kanis, M. A. Ratner, T. J. Marks, *Chem. Rev.* **1994**, *94*, 195; b) L. R. Dalton, A. W. Harper, R. Ghosn, W. H. Steier, M. Ziari, H. Fetterman, Y. Shi, R. V. Mustacich, A. K. Y. Jen, K. J. Shea, *Chem. Mater.* **1995**, *7*, 1060; c) F. Würthner, R. Wortmann, K. Meerholz, *ChemPhysChem* **2002**, *3*, 17.
- [2] a) A. Mishra, P. Bäuerle, *Angew. Chem. Int. Ed.* **2012**, *51*, 2020; b) Y. Lin, Y. Li, X. Zhan, *Chem. Soc. Rev.* **2012**, *41*, 4245; c) B. Walker, C. Kim, T.-Q. Nguyen, *Chem. Mater.* **2011**, *23*, 470; d) Y. Li, Q. Guo, Z. Li, J. Pei, W. Tian, *Energy Environ. Sci.* **2010**, *3*, 1427; e) J. Roncali, *Acc. Chem. Res.* **2009**, *42*, 1719.
- [3] F. Würthner, K. Meerholz, *Chem. Eur. J.* **2010**, *16*, 9366.
- [4] a) H. Bürckstümmer, E. V. Tulyakova, M. Deppisch, M. R. Lenze, N. M. Kronenberg, M. Gsänger, M. Stolte, K. Meerholz, F. Würthner, *Angew. Chem. Int. Ed.* **2011**, *50*, 11628; b) A. Ojala, H. Bürckstümmer, M. Stolte, R. Sens, H. Reichelt, P. Erk, J. Hwang, D. Hertel, K. Meerholz, F. Würthner, *Adv. Mater.* **2011**, *23*, 5398.
- [5] a) H.-W. Lin, L.-Y. Lin, Y.-H. Chen, C.-W. Chen, Y.-T. Lin, S.-W. Chiu, K.-T. Wong, *Chem. Commun.* **2011**, *47*, 7872; b) S.-W. Chui, L.-Y. Lin, H.-W. Lin, Y.-H. Chen, Z.-Y. Hunag, Y.-T. Lin, F. Lin, Y.-H. Liu, K.-T. Wong, *Chem. Commun.* **2012**, *48*, 1857; c) Y.-H. Chen, L.-Y. Lin, C.-W. Lu, F. Lin, Z.-Y. Huang, H.-W. Lin, P.-H. Wang, Y.-H. Liu, K.-T. Wong, J. Wen, D. J. Miller, S. B. Darling, *J. Am. Chem. Soc.* **2012**, *134*, 13616.
- [6] a) A. Leliège, C.-H. Le Régent, M. Allain, P. Blanchard, J. Roncali, *Chem. Commun.* **2012**, *48*, 8907; b) D. Demeter, T. Rousseau, J. Roncali, *RSC Adv.* **2013**, *3*, 704; c) V. Jeux, D. Demeter, P. Lzeriche, J. Roncali, *RSC Adv.* **2013**, DOI: 10.1039/c3ra40966.
- [7] a) H. Brisset, C. Thobie-Gautier, A. Gorgues, M. Jubault, J. Roncali, *J. Chem. Soc. Chem. Commun.* **1994**, 1765; b) J. Roncali, C. Thobie-Gautier, *Adv. Mater.* **1994**, *6*, 846; c) P. Blanchard, H. Brisset, A. Riou, J. Roncali, *J. Org. Chem.* **1997**, *62*, 2401; d) P. Blanchard, P. Verlhac, L. Michaux, P. Frère, J. Roncali, *Chem. Eur. J.* **2006**, *12*, 1244; e) J. M. Raimundo, P. Blanchard, N. Gallego-Planas, N. Mercier, I. Ledoux-Rak, R. Hierle, J. Roncali, *J. Org. Chem.* **2002**, *67*, 205.
- [8] a) Z. Liu, R. C. Larock, *J. Org. Chem.* **2006**, *71*, 3198; b) C. Teng, X. Yang, C. Yang, S. Li, M. Cheng, A. Hagfeldt, L. Sun, *J. Phys. Chem. C* **2010**, *114*, 9101.
- [9] L. Y. Lin, C. H. Tsai, F. Lin, T. W. Huang, S. H. Chou, C. C. Wu, K. T. Wong, *Tetrahedron* **2012**, *68*, 7509.
- [10] Q.-Y. Yu, J.-Y. Liao, S.-M. Zhou, Y. Shen, J.-M. Liu, D.-B. Kuang, C.-Y. Su, *J. Phys. Chem. C* **2011**, *115*, 22002.
- [11] a) O. Meth-Cohn, S. Gronowitz, *Acta Chem. Scand.* **1966**, *20*, 1577; b) D. B. Hauze, M. M. Joullie, *Tetrahedron* **1997**, *53*, 4239.
- [12] G. Qian, B. Dai, M. Luo, D. Yu, J. Zhan, Z. Zhang, D. Ma, Z. Y. Wang, *Chem. Mater.* **2008**, *20*, 6208.
- [13] a) S. Roquet, A. Cravino, P. Leriche, O. Alévêque, P. Frère, J. Roncali, *J. Am. Chem. Soc.* **2006**, *128*, 3459; b) E. Ripaud, Y. Olivier, P. Leriche, J. Cornil, J. Roncali, *J. Phys. Chem. B* **2011**, *115*, 9379; c) Y. Lin, Z.-G. Zhang, Y. Li, D. Zhu, X. Zhan, *J. Mater. Chem.* **2013**, DOI:10.1039/C3TA10205J.
- [14] J. Roncali, *Chem. Rev.* **1997**, *97*, 173.
- [15] A. Leliège, D. Demeter, T. Rousseau, P. Blanchard, J. Roncali, unpublished.
- [16] P. Peumans, S. Ushida, S. R. Forrest, *Nature* **2003**, *425*, 158.
- [17] D. Demeter, T. Rousseau, P. Leriche, T. Cauchy, R. Po, J. Roncali, *Adv. Funct. Mater.* **2011**, *21*, 4379.
- [18] R. Fitzner, E. Reinold, A. Mishra, E. Mena-Osteritz, H. Ziehkle, C. Korner, K. Leo, M. Riede, M. Weil, O. Tsaryova, A. Weiss, C. Ulrich, M. Pfeiffer, P. Bäuerle, *Adv. Funct. Mater.* **2011**, *21*, 897.
- [19] E. Ripaud, T. Rousseau, P. Leriche, J. Roncali, *Adv. Energy Mater.* **2011**, *1*, 540.